Comparison of Strain-Rate Maps of Western North America

Authors:
David Sandwell, Scripps Institution of Oceanography
Thorsten Becker, University of Southern California
Peter Bird, University of California at Los Angeles
Yuri Fialko, Scripps Institution of Oceanography
Andrew Freed, Purdue University
William Holt, State University of New Yory, Stony Brook
Corne Kreemer, University of Nevada
Jack Loveless, Harvard University
Brendan Meade, Harvard University
Rob McCaffrey, Rensselaer Polytechnic Institute
Fred Pollitz, USGS Menlo Park
Bridget Smith-Konter, University of Texas at El Paso
Yuehua Zeng, USGS, Golden, CO

Abstract:
GPS measurements across the North American - Pacific Plate boundary are providing decade and longer time series at 2 to 3 millimeter-level precision from which surface velocity estimates are derived. Several geodetic research groups have used these point velocity measurements to construct large-scale maps of crustal strain rate. Since the typical spacing of GPS stations is 10 km or greater, an interpolation method or physical model must be used to compute a continuous vector velocity model that can be differentiated to construct a strain-rate map. Four approaches are used to develop strain maps: isotropic interpolation, interpolation guided by known faults, interpolation of a rheologically-layered lithosphere, and analytically determined strain rates derived from a geodetically constrained block model in an elastic half space. This poster compares the strain-rate maps of several groups using these different methods to define common features as well as differences among the maps. The differences reveal the spatial resolution limitations of GPS arrays, as well as assumed fault locations and the effects of differing assumptions about crustal rheology. Moreover the comparisons promote collaboration among the various groups to develop the best possible strain-rate map. Our first analysis only compares the magnitude of the strain rate given by the following formula sqrt(exx*exx +eyy*eyy+2*exy*exy)..

References (incomplete):
Bird,P.[2007] Uncertainties in long-term geologic offset rates of faults: General principles illustrated with data from California and other western states, Geosphere, 3(6), 577-595, doi:10.1130/GES00127.1, + 9 digital file appendices.
Bird,P., Long-term fault slip rates, distributed deformation rates, and forecast of seismicity in the western United States from joint fitting of community geologic, geodetic, and stress-direction datasets, submitted to J. Geophys. Res., 2009.
Freed,A.M., S.T.All, and R.Bürgmann, Evolution of stress in Southern California for the past 200 years from coseismic, postseismic and interseismic stress changes, Geophys. J. Int., v. 169, p. 1164-1179, 2007.
Gonzalez-Garcia,J. J. L. Prawirodirdjo, Y. Bock, and D. Agnew [2003] Guadalupe Island, Mexico as a new constraint for Pacific plate motion, Geophys. Res. Lett., 30(16), 1872, doi: 10.1029/2003GL017732.
Lyons, S. N., Y. Bock, and D. Sandwell, Creep along the Imperial fault, southern California, from GPS measurements, J. Geophys. Res., 107(B10), 2249, doi:10.1029/2001JB000763, 2002.
Parsons, T., Tectonic stressing in California modeled from GPS observations, J. Geophys. Res. 111, doi:10.1029/2005JB003946 (2006).
Payne, S. J., McCarey, R., and King, R. W., 1996. Strain rates and contemporary deformation in the Snake River Plain and surrounding Basin and Range from GPS and seismicity. Geology, 36, 647-650.
Platt, J. P., B. Kaus, and T. Becker, The mechanics of continental transforms: An alternative approach with applications to the San Andreas system and the tectonics of California, Earth Planet. Sci. Lett., v. 274, p. 380-391, 2008.
Shen, Z.-K., Jackson, D. & Ge, B., 1996. Crustal deformation across and beyond the Los Angeles Basin from geodetic measurements, J. Geophys. Res., 101, 27957-27980.
Shewchuk, J. R., 1996, Triangle: Engineering a 2D Quality Mesh Generator and Delaunay Triangulator, First Workshop on Applied Computational Geometry (Philadelphia, PA), 124-133.
Smith-Konter, B. and D. Sandwell, Stress evolution the San Andreas Fault System: Recurrence interval versus locking depth, Geophys. Res., Lett., in press, 2009.
Smith, B., and D.T. Sandwell, A model of the earthquake cycle along the San Andreas Fault System for the past 1000 years, J. Geophys. Res. 111, doi:10.1029/2005JB003703 (2006).
Wdowinski, S., Y. Sudman, and Y. Bock (2001), Geodetic detection of active faults in S. California, Geophys. Res. Lett., 28, 2321-2324.
Wdowinski, S., B. Smith-Konter, Y. Bock, and D.T. Sandwell, Spatial characterization of the interseismic velocity field in southern California, Geology, doi:10.1130/G22938A.1 (2007).

long-term crustal strain

bird

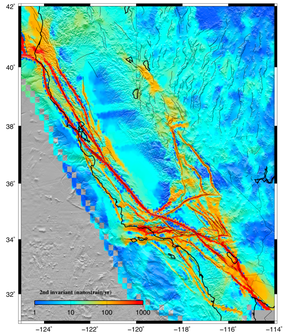

Estimated long-term-average strain-rates [Bird, 2009]. (These include mean rates of fault-ing, but do not include any elastic strain accumulation. Distributed deformation predicted away from mapped faults may reflect other faults not yet modeled.) Computed with 2-D kinematic F-E code NeoKinema from community datasets including: 248 WGCEP fault traces in CA and 1231 fault traces in other states or offshore, 572 PaleoSites/Bird [2007] fault offset rates and 126 newer rates from literature, 1226 GPS velocities in CA from Shen et al. [2009] and 193 PBO GPS velocities in other western states, 2068 stress-direction indicators from the World Stress Map, and the Gonzalez-Garcia et al. [2003] Euler pole for NA-PA. Model assumes that GPS velocities are from interseismic periods, and corrects interseismic velocities to long-term velocities using traditional dislocation-in-elastic-halfspace corrections, in a self-consistent (iterated) way.

becker

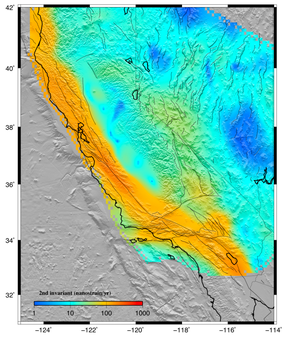

Crustal strain-rates based on a high quality subset of the 2007 release of the horizontal GPS velocity solution from EarthScope PBO. Processing assumes continuous deformation, uses modified Generic Mapping Tool software, and strives for a smooth representation of the velocity gradients (see Platt et al, EPSL, 2008, for details).

fialko

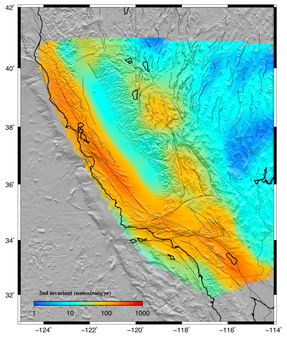

The second invariant of the strain rate tensor is calculated from a set of 722 continuous GPS sites within the area of interest for which velocity solutions are available from either SOPAC or PBO. The two horizontal velocity components were first approximated on a regular grid by least-square fitting of a smooth surface using a modified ridge estimator. The resulting velocity fields were differentiated to obtain components of the strain rate tensor. A Gaussian low-pass filter of size 0.75 degrees and standard deviation of 0.25 degrees was applied to the calculated second invariant of the strain rate.

freed

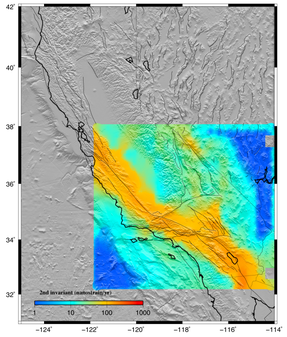

Strain rates were derived based on 810 SCEC 3 velocity vectors (http://epicenter.usc.edu/cmm3.0). We linearly interpolated the velocity data to an evenly spaced grid with increments of 0.1 degrees across the region using a weighted nearest neighboring scheme to dampen any locally sharp velocity contrasts. For grid points outside of the SCEC 3 region, we extrapolated the velocity field based on a fixed North America plate and a Pacific plate with a velocity of 48 mm/yr. We then triangulated the evenly spaced grid points using Delaunay triangulation (e.g., Shewchuk, 1996), and the strain tensor is determined for each triangle using minimum norm least squares. Reference: Freed et al., 2007.

harvard

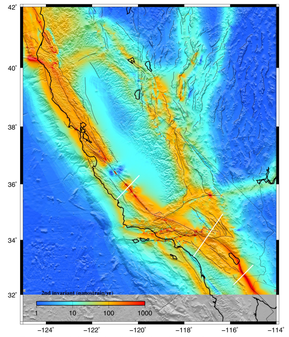

The strains are calculated analytically using elastic dislocation theory in a homogeneous elastic halfspace. The model is subset of a western US block model geodetically constrained by a combination of the SCEC CMM 3.0, McClusky ECSZ, Hammond Walker Lane, McCaffrey PNW, d'Alessio Bay Area, and PBO velocity fields. These are combined by minimizing residuals (6-parameter) at collocated stations. In southern California the block geometry is based on and the Plesch et al., CFM-R and features dipping faults in the greater Los Angeles regions which end up producing some intricate strain rate patterns. The model features fully coupled (locked from the surface to some locking depth) faults everywhere except for Parkfield, the SAF just north, and the Cascadia subduction zone. For Parkfield and Cascadia we solve for smoothly varying slip on surfaces parameterized using triangular dislocation elements.

holt

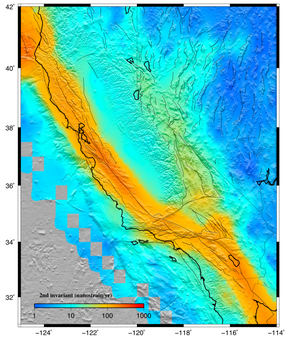

Second invariant of strain rate obtained from bi-cubic spline interpolation of 4948 campaign and EarthScope PBO GPS velocities. Model parameters are estimated through a weighted least-squares inversion of the GPS within a grid region extending from Alaska to the Rivera Plate. The reference frame for each GPS study was solved for in the inversion in order to place all observations into a best fit North America model reference frame.

kreemer

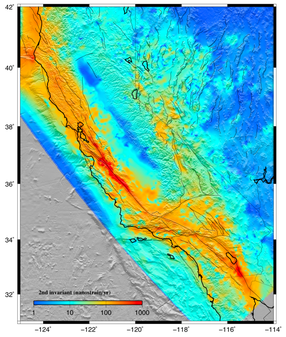

Strain rate tensor model derived from fitting a continuous horizontal velocity field through GPS velocities (Kreemer et al, 2009, this meeting). 2053 GPS velocities were used, of which 854 from our own analysis of (semi-)continuous sites and 1199 from published campaign measurements (all transformed into the same reference frame). The model assumes that the deformation is accommodated continuously, and lateral variation in damping is applied to ensure that the reduced chi^2 fit between observed and modeled velocities is ~1.0 for subregions.

mccaffrey

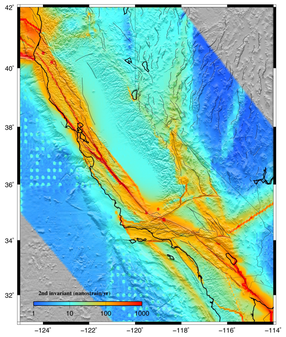

Model of horizontal surface velocities (converted to strain) for the western United States. While there are many ways to go about doing this, here we have chosen to generate a geologic block model, constrained by observations from geodesy, seismology and geology. The parameters of the block model are constrained by non-linear least-squares inversion. The locking depth is set to 10 km for segments where locking depth is not well constrained by GPS. The model is used to predict surface velocity on a uniform grid at 0.02 degree spacing. Grids were filtered at 0.5 gain at 10 km wavelength.

pollitz

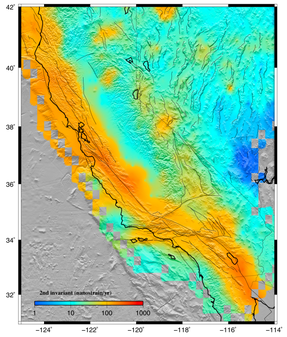

Strain rates are derived by applying the isotropic interpolation method of Shen et al. (1996) to a compilation of 3650 horizontal GPS vectors in the western US. Contributing sources include PBO (714 vectors), Payne et al. (2008) (672 vectors), and various continuous and campaign GPS measurements (2264 vectors) such as USGS campaign data and the SCEC Crustal Motion Model 3.0. The Gaussian scaling distance used to weight velocity information in the Shen et al. method is here implemented as a function of position depending on the density of GPS measurements around a target point. This varies from 12 km in densely covered areas to 50 km in sparsely covered areas.

smith_konter

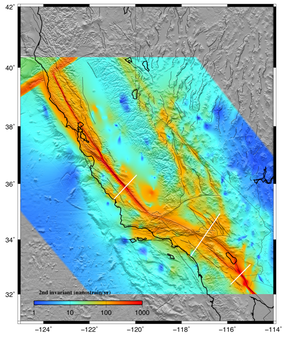

Strain rate derived from a dislocation model of the San Andreas Fault system [Smith-Konter and Sandwell, GRL, 2009]. 1709 GPS velocity vectors were used to develop the model. The model consists of an elastic plate over a visco-elastic half space at 1 km horizontal resolution. Deep slip occurs on 41 major fault segments where rate is largely derived from geological studies. The locking depth is varied along each fault segment to provide a best fit to the GPS data. The model is fully 3-D and the vertical component of the PBO GPS vectors is also used in the adjustment. Since the dislocation model cannot capture all the tectonic and non-tectonic motions, especially in areas away from model fault segments, we fit the horizontal GPS residuals (40 km blockmedian) to a biharmonic spline using a tension factor of 0.45 weighted by the uncertainty in each GPS data point. After fitting the residual GPS velocities misfit is 1.47 mm/yr in the E-W direction, 1.56 mm/yr and 2.73 mm/yr in the up direction.

zeng

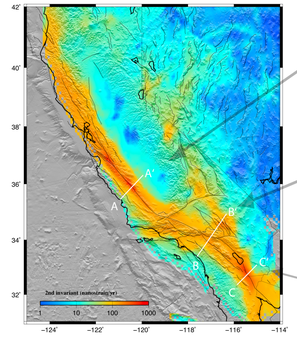

The GPS data for the western US are obtained from PBO velocity at UNAVCO site, Southern California Earthquake Center California Crustal Motion Map 1.0, McCaffrey et al. (2007) for Pacific Northwest, the GPS velocity field of Nevada and its surrounding area from the Nevada Geodetic Lab at the University of Nevada at Reno, and the GPS velocity field of the Wasatch-Front and the Yellowstone-Snake-River-River-Plain network from Bob Smith of University of Utah. These separate velocity fields are combined by adjusting their reference frames to make velocities match at collocated stations. I determined the Voronoi cells for this combined GPS stations and used their areas to weight the corresponding stations for inversion. I then interpolated those GPS observation into uniform grid point for the western US using the method of Wald (1998) and calculated the final strain rate map.

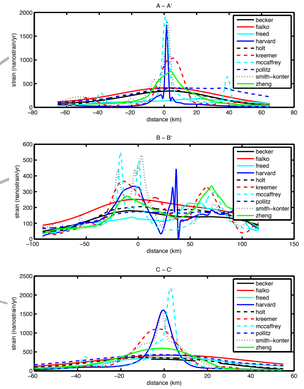

Conclusions:

Strain rates differ by a factor of 5-8 depending on methods used. The greatest differences occur within 15 km of the San Andreas Fault system.

Isotropic gridding of sparse PBO GPS data (10-15 km spacing) results in low strain rate.
Enhanced gridding of higher density GPS data results in intermediate strain.
Dislocation modeling with variable locking depth results in high strain rate near faults.

Interseismic stress accumulation rate is proportional strain accumulation rate so the is no consensus on stress accumulation rates along major faults.

Accurate measurements of stress accumulation rates are essential for understanding the earthquake cycle so order of magnitude differences reveals a weakness in the PBO.

Augmentation of the PBO array with dense campaign GPS profiles and L-band radar interferometry is needed to improve stress accumulation rate measurements near major faults.